6
Water Treatment: Removal of Cr(VI) and Organic Contaminants

In the rapidly developing world, with new technological and increasing world population, more energy is being required and consumed about 25.8 TW by 2035. To meet this goal there will be severe consequences, pollution, especially water and air pollution are expected to rise significantly. Sudden changes in weather, global warming, industrial developments, growing population and many more are the key factors for the shortage of clean water over the world. Mostly natural resources like the river is polluted with containments produced by domestic or industrial waste and limits the usage of one of the big natural source of water. By 2025, almost all countries (2/3) in the world will be struggling for clean water, to tackle this problem, water treatments and purification are a prominent answer to reuse this contaminated water and decreases water shortage [Liu, *et al.*, 2016]. The source of very harmful contaminants like chromium are mainly produced by leather tanning, mining pigment manufacturing and electroplating processes [Challagulla, *et al.*, 2016]. The Cr(VI) is always proven to be more dangerous than Cr(III), it is xenotoxic carcinogenic. It mainly targets the respiratory organ, kidney, liver and even damages blood cells due to its oxidative nature [Li, *et al.*, 2016]. The safety limits acknowledged by world health organization approves 50 µg/L quantity of Cr(VI) in drinking water. The existing purification techniques could report higher efficiency but simultaneously their higher cost and harmful secondary contamination limit its application [Neagu and Mikhalovsky, 2010; Naushad, *et al.*, 2015; Sun, *et al.*, 2014].

The massive amount of clean solar energy falls on earth surface every year, which is very abundant, sustainable and most important it is free. Recently, it has been attracted researchers towards utilization of solar energy in water treatment. Photocatalysis has been proven as a clean technology for water treatment on large scale. In the process, the photocatalytic material absorbs the light and generates $OH\bullet$, $O_2\bullet-$, H_2O_2 and O_3 species [Dong, Feng, Fan, Pi, Hu, Han, Liu, Sun and Sun, 2015; Fan, *et al.*, 2015; Gaya and Abdullah, 2008], which can degrade harmful contaminants in nonharmful as shown in Figure 6.1.

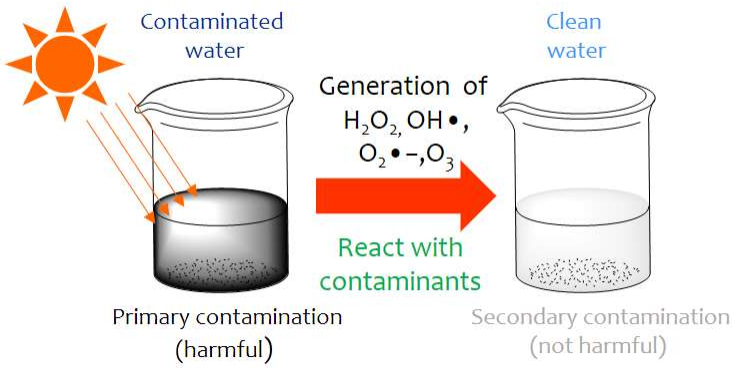

Figure 6.1 : World energy demand by energy source

Mostly study is focused on the low band gap material to cover wide spectrum of light and efficient catalyst like $BaTiO_3$, $SrTiO_3$, $BiWO_6$, In_2S_3, CdS and AgI [Peng, *et al.*, 2013; Sambandam, *et al.*, 2015; Torres-Martínez, *et al.*, 2013; Yang, *et al.*, 2015]. Eventually, the highly efficient catalyst will always have cost constraint and their preparation process includes various tedious steps like high pressure, temperature and rear earth metals which make them more cumbersome. The catalyst can be effectively used in a specific range of the solar spectrum like UV light and visible light source. In case of organic pollutants, with less concentration UV light is quite sufficient for degradation of all contaminants from water, whereas the percentage of UV light is only of about 4-5% of the total solar spectrum [Goslich, *et al.*, 1997].

The titanium dioxide has been explored extensively as good photocatalyst material to remove highly toxic pollutants in water due to its nontoxic, low-cost, stable and abundance nature. With a wide band gap of 3.2 eV, it efficiently works in UV and near UV region of sunlight and eventually exhibits lower photocatalytic efficiency. There have been extensive study on the modification of morphology, composition, doping and structure to increase its photocatalytic activity [Pan, *et al.*, 2011]. Even through material band gap engineering, the usage of the photon in the full spectrum showed enhancement in efficiency. Other promising route to utilize solar energy for water purification is evaporation, water is evaporated with degradation of contaminants where thermal energy is used for the process [Meziani, *et al.*, 2016; Manshor, *et al.*, 2016].

The degradation efficiency can be increased by the raising photocatalyst concertation, but it drastically enhances the cost of the system, mostly these high-efficiency photocatalysts are expensive to prepare. With low contaminates, a small amount of catalyst is proven to be an ideal system but as the catalytic site are less, degradation period will be lengthened. To resolve this issue, a system with more sites for trapping contaminants to enhance interaction between the catalyst and contaminates will have good potential even with less amount of catalyst.

6.1 PHOTO-CATALYTIC MEMBRANE

6.1.1 Fabrication and Morphology

In this work, catalytic nanoparticles are embedded in the membrane by a simple fabrication process. This novel design facilitates more surface for trapping contaminants and purifies the water by solar driven catalytic degradation.

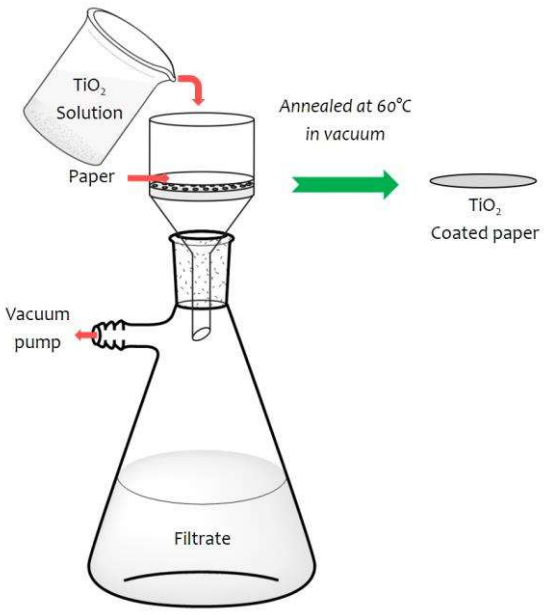

Figure 6.2 : Schematic illustration of photocatalytic membrane fabrication

The system is composed of simple Whatman filter paper as supporting membrane for more trapping sites and catalytic materials decorated all over the membrane as shown in Figure 6.2 Briefly, titania (catalytic material) decorated filter membrane was prepared by filtration of solution contains titania prepared at subzero temperatures, distilled water and surfactant. This composite membrane was thoroughly washed with distilled water for several times and dried at 60°C under air condition for 12 hours and then used as a photo-assisted membrane to remove organic impurities and toxic materials from water.

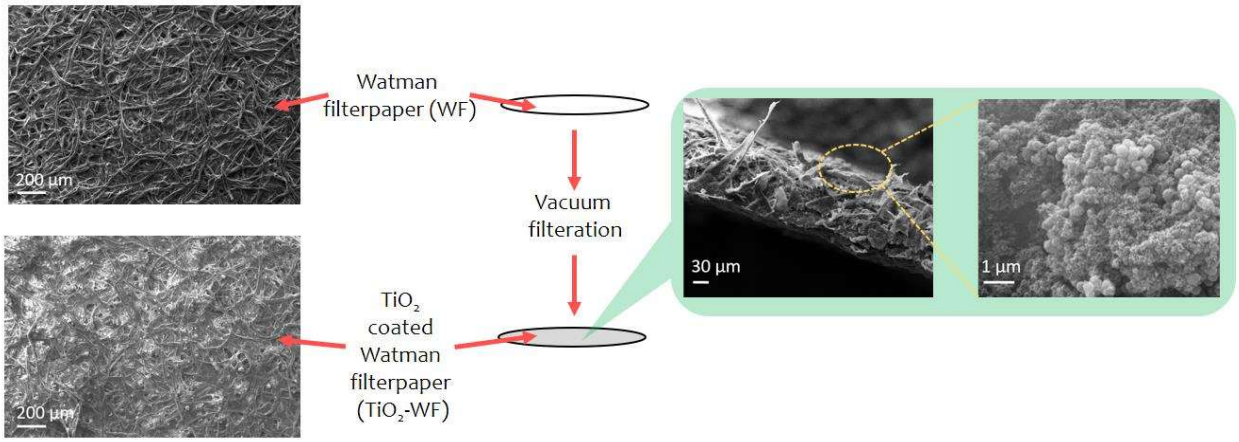

Figure 6.3 : SEM images of blank and TiO_2 coated filter paper/membrane and inset shows cross-sectional SEM images of TiO_2 coated filter membrane.

The blank and TiO_2 coated filter papers were visualized by SEM and shown at left portion of Figure 6.3. The TiO_2 as a catalytic material formed a uniform and densely packed layer all over the porous filterpaper (see inset of Figure 6.3). The particle size of TiO_2 (sub-zero temperature TiO_2, ZnO-TiO_2 and HfO_2/TiO_2 nanosphere) was less than 300 nm, which is unable to block the pores membrane and this can be seen in Figure 6.3. This porous structure also helps in minimizing TiO_2 loss during water treatment. Compared to other techniques, this approach of photo-assisted TiO_2 filter membrane for water purification is simple, fast, cost-effective, reusable and more importantly have wide application in the large area [Xia and Brueck, 2004; Rabani, *et al.*, 2003; Xia, *et al.*, 2004]. Also, this flexible TiO_2 water filter membrane could be useful in solar driven evaporation and various sensors. The morphology of such membrane helps the solar light to penetrate and have more interaction with the water-contaminant complex and degrade them into nonharmful byproducts. Upon solar light irradiation, the photocatalytic membrane starts degrading contaminants from the water, the heat gradient could be the driving force to circulate water towards the membrane.

6.1.2 Restoration of photo-catalytic membrane

Whatman filter paper is used as a substrate for loading the photocatayst synthesized to be used in photo reductive water treatment.

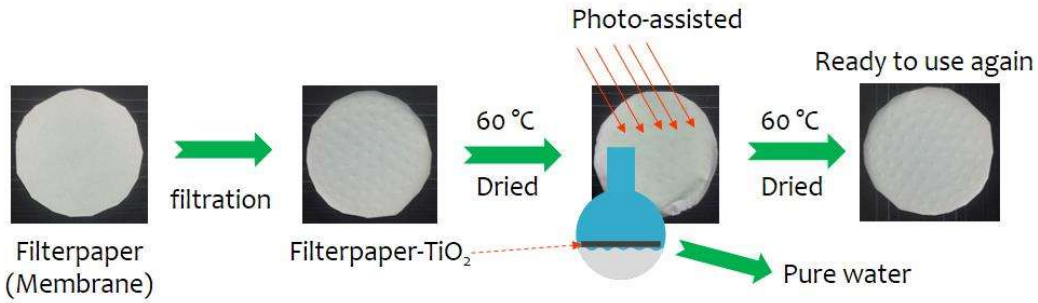

Figure 6.4 : Photographic stepwise illustration of photo-catalytic membrane restored using 1 sun radiation

The photocatalyst is loaded by means of a passing photocatalyst contained distilled water over the filter paper. The filter paper is dried under vacuum at a temperature of 60°C. The contaminated water that needs to be treated is then taken in a beaker along with the loaded filter paper and is kept exposed under irradiation. Due to heating, a thermal cycle is the driving for the water movement. Thus, after a certain exposure time the water is completely free of the contaminants. The filter paper is dried under vacuum for a period of 12 hours at 60°C to be used for the next cycle (see Figure 6.4).

6.2 PHOTO ASSISTED Cr(VI) REDUCTION

6.2.1 Sub-zero temperature TiO_2 membrane and reaction rate

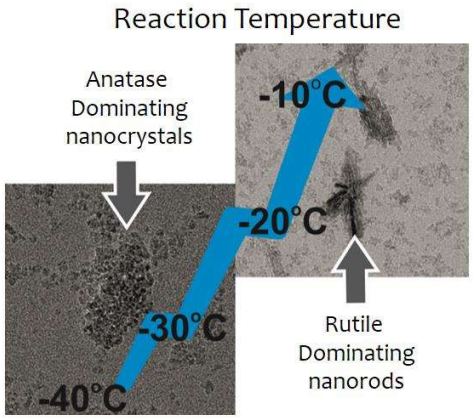

Figure 6.5 : HRTEM images of sub-zero temperature synthesized at -10 and -40°C

The photocatalytic activity of the sub-zero temperature synthesized at -10 to -40°C are used for photocatalyst material for evaluation of photo-assisted Cr(VI) reduction (see Figure 6.5). The conversion rate of Cr(VI) for the -40°C was the highest followed by -30, -20 and -10°C. After a time interval of 60 minutes light irradiation the Cr(VI) removal was 50% for the -40°C system while only 20% was reduced by the -10°C system. The -30 and -20°C reduced about only 30-35% of Cr(VI) after 60 minutes into the reaction. Also, -40°C showed best Cr(VI) by the end of the reaction at 120 minutes where it reduced the Cr(VI) level by ~ 75% as shown in Figure 6.6a.

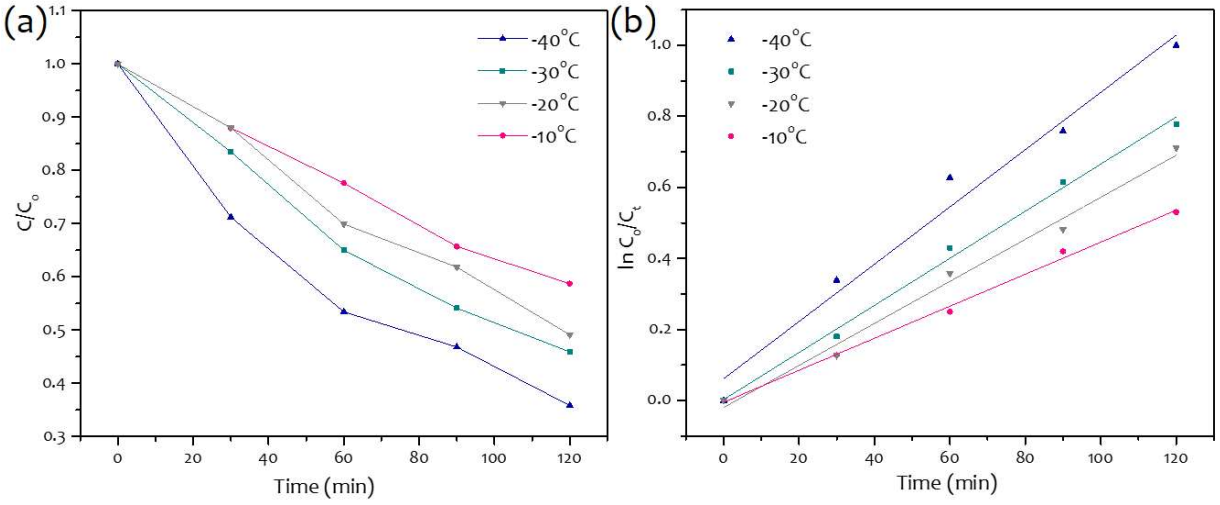

Figure 6.6 : Comparison of (a) photocatalytic activities and (b) rate constant of sub-zero temperature (-40 to -10°C) photo-catalytic membrane

This result could be influenced by the fact that the -40°C system consists of anatase dominating phase with lesser rutile concentration while the -10°C has rutile as the dominating phase with lesser anatase concentration as shown in Figure 6.5. Thus, the anatase concentrated system provided better Cr(VI) reduction and decreases with increase in rutile concentration. Above this, the -40°C has nanocrystals with oval shaped morphology in contrast to -10°C having nanorods. This greatly influence surface area of the material with 135 $m^2 g^{-1}$ for the -40°C and 100 $m^2 g^{-1}$ for -10°C sample (as previously discussed in Chapter 3) and thereby affecting the extent of Cr(VI) removal. The photocatalytic activity of the sub-zero temperature TiO_2 membrane is calculated by analyzing the reaction rate contact (k). This photocatalytic degradation of Cr(VI) is a pseudo-first order reaction and it follows Langmuir–Hinshelwood kinetic model, $\ln(C_0/C_t) = kt$, where the C_o is the initial concentration and C_t is the concertation of contaminant after t minutes of irradiation. A plot of $\ln(C_0/C_t)$ Vs time is a straight line with a positive slope is plotted for the four synthesized materials. Under one sun solar irradiation, the rate constant for the removal of Cr(VI) is 0.0087, 0.0066, 0.0059 and 0.0045 min^{-1} for TiO_2 prepared at -40 to -10°C respectively, as shown in Figure 6.6b. The more active sites clearly show significant enhancement in the reaction rate at -40°C which possesses highest surface area among all, and then start decreasing with respect to surface area.

6.2.2 ZnO-TiO_2 nanosphere and reproducibility

Briefly, TiO_2 having anatase phase was synthesized. As a modification to this system, TiO_2 was mixed with ZnO forming type II heterojunction which was realized with the help of a hydrothermal reaction (see Figure 6.7).

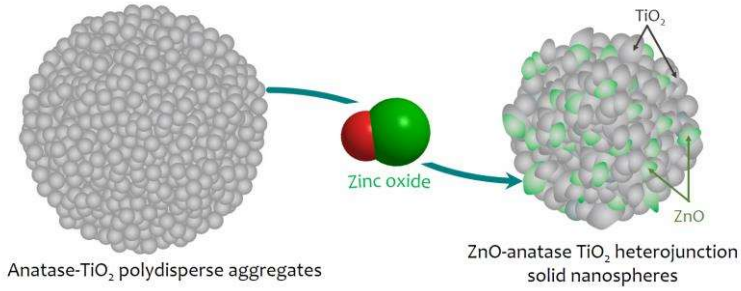

Figure 6.7 : Schematic illustration of ZnO-TiO_2 heterojunction solid nanospheres morphology

This is a spherical shaped structure consisting of TiO_2 and ZnO nanocrystals giving rise to a highly porous assembly with enhanced light trapping effects leading up to good electron carrier density when tested as a photoanode material for DSSC. Now, to observe its activity, it is utilized as a photocatalyst for dye degradation.

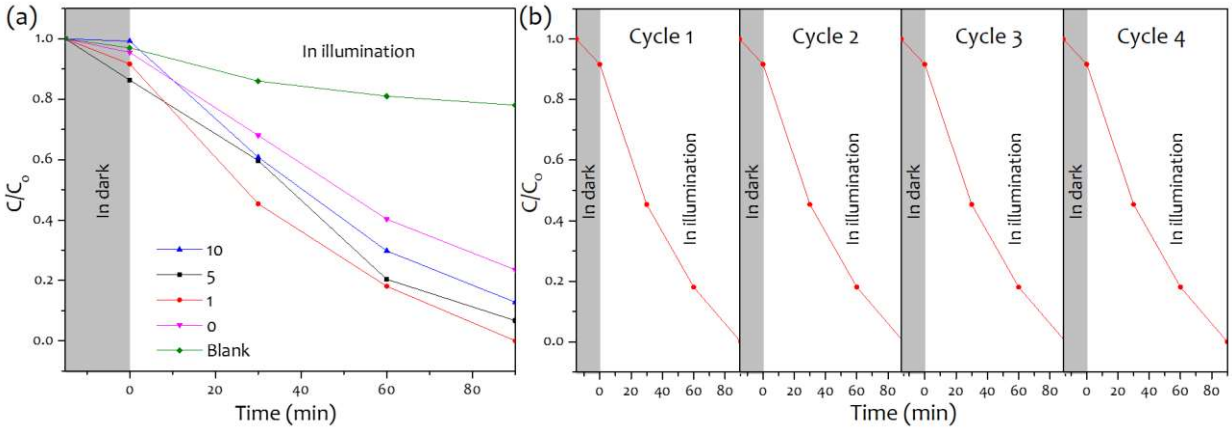

Figure 6.8 : Comparison of (a) photocatalytic activities and (b) photoreduction up to four cycles of 0 to 10% ZnO-TiO_2 photo-catalytic membrane

The change of ratio C/C_O vs time on irradiation with light is shown in Figure 6.8a. This measurement was taken using the filtration method where a filter paper embedded with the nanomaterials synthesized is kept and the Cr(VI) contaminated water is made to pass through the filter paper. In all the experiments, 15 min in dark condition was set to obtain equilibrate of adsorption/desorption process on the filter membrane. Blank experiments were performed to suggest that the change in concentration of the Cr(VI) does not change without the effect of the presence of photocatalyst under light irradiation. It can be observed that the 1% ZnO doped TiO_2 showed fast removal and degradation of Cr(VI) and almost 80% is removed 60 minutes after the start of the reaction. The undoped TiO_2 showed least amount of Cr(VI) removal. Also, the increase in doping does not increase the removal as is observed in the Figure 6.8a that the 5% and 10% ZnO doped TiO_2 does not remove Cr(VI) to the extent of 1%.

To observe the photo-stability and the reusability of the synthesized nanomaterials as photocatalyst a cyclic test was performed as shown in Figure 6.8b. The filter membrane loaded with the nanomaterials did not show any significant decrease in the performance even after the end of four cycles. The 1% ZnO doped TiO_2 was able to degrade more than 95% of Cr(VI) in 80 minutes for continuous four cycles. The slight decrease in the performance may be because of less number of the reactive site were available due to adsorption of contaminants on the reactive sites of the membrane.

6.2.3 H-HfO_2/TiO_2 and industrial organic dye impurities

TiO_2 is one of the most extensively used semiconductor for its good stability, non-toxicity and abundance. Apart from this, TiO_2 is a wide band gap semiconductor absorbing at 3.2 eV which corresponds to absorption at UV wavelength. But sadly, UV covers only a trifling portion which is about 4% of the total spectrum that the earth receives. In order to fully utilized the solar spectrum, it is important to tune the band gap of TiO_2 such that it absorbs the maximum portion covered by the visible spectrum in the solar spectrum. Thus, TiO_2 is engineered to tune its band gap.

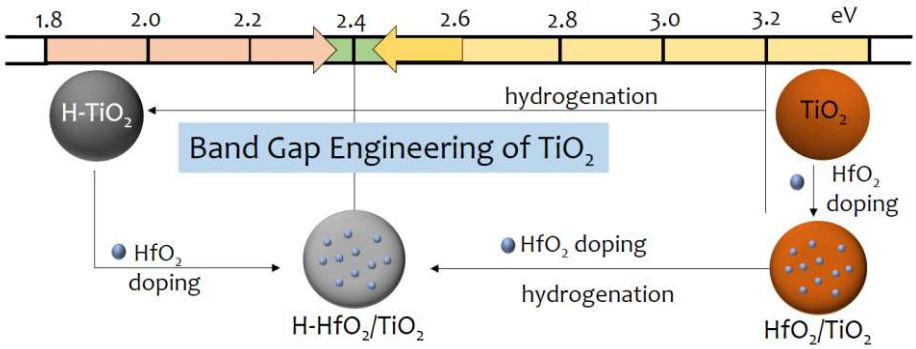

Figure 6.9 : Schematic illustration of the band gap engineering of TiO_2 nanospheres by hydrogenation and doping with HfO_2 nanodots

Most common method is via doping. The TiO_2 when it is annealed under the influence of hydrogen has bandgap reduced to about 1.8 eV. But reducing it to this amount also will mean that there will be greater charge recombination after photoexcitation of the charge carriers. On the other hand, when TiO_2 is doped by 1% HfO_2, the HfO_2 does not show much effect to change the bandgap. But when the HfO_2/TiO_2 is annealed under H_2 then the band gap is reduced to an optimum level of 2.4 eV. This shows that these new materials will absorb at about 520 nm wavelength which clearly falls in the visible range. Thus, the band gap of TiO_2 is engineered as shown in Figure 6.9.

Photocatalytic degradation of several industrial dyes – methyl orange, methylene blue, cresol red, solochrome black and thymol blue are very burning problem in water treatment as its very hazardous pollutant and mostly contaminant the large quantity of water (see Figure

6.10). So, to solve this issue photo-catalysis has been used to degrade these dyes and purify the water. In this process, the contaminated water along with the photocatalyst is exposed to sunlight under stirring on a hot plate. After certain time of exposure, the sunlight along with the photocatalyst helps degrade the harmful contaminants in the water.

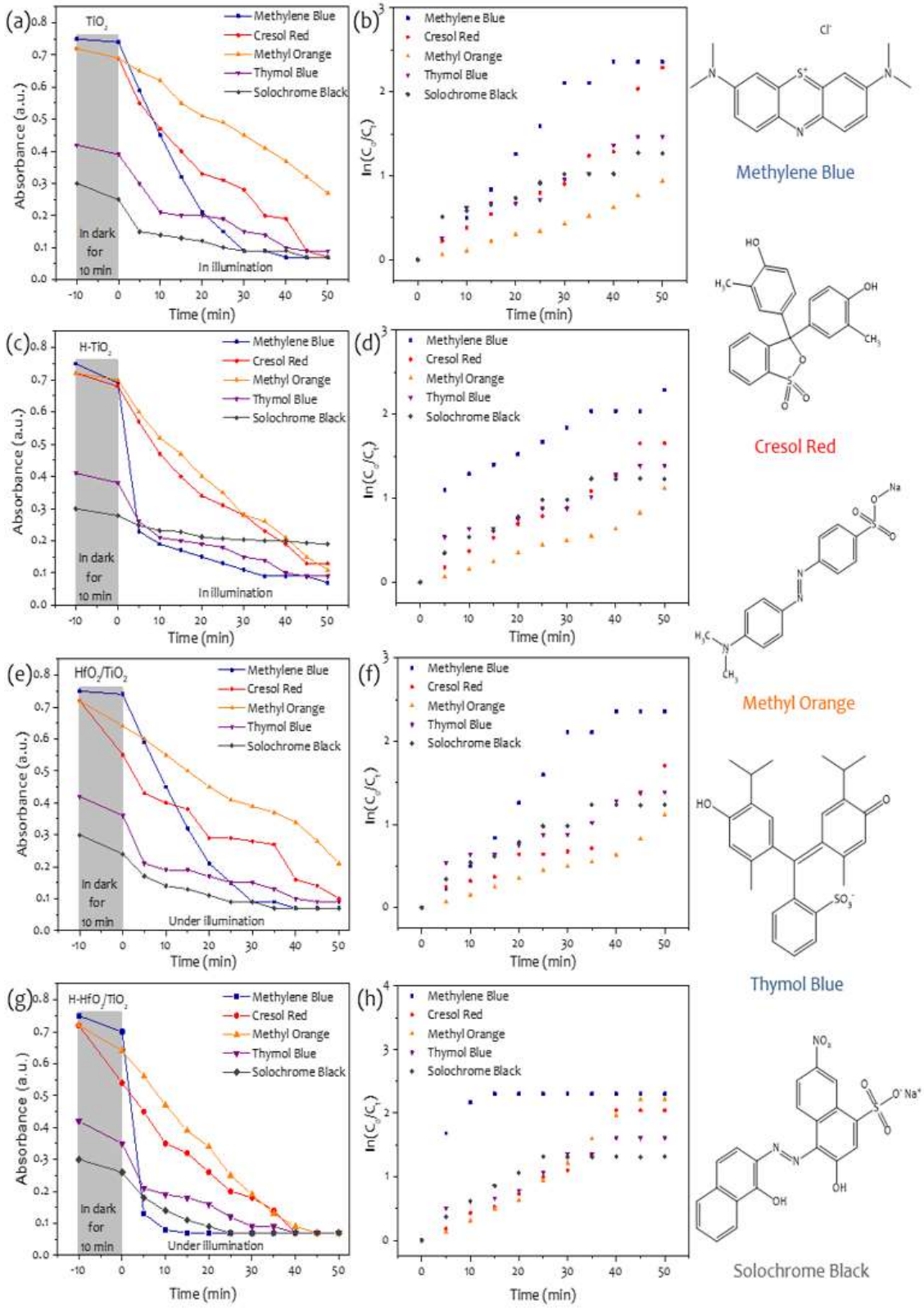

Figure 6.10 : (a) – (b), (c) – (d), (e) – (f) and (g) – (h) are photocatalytic activities – reaction of TiO_2, H-TiO_2, HfO_2/TiO_2 and H-HfO_2/TiO_2 respectively, and left portion of figure shows chemical structure of all dyes

During the entire time of reaction, the progress was monitored using a colorimetry instrument. The effect of the photocatalyst was measured for a total of 60 minutes throughout which at a time interval of 5 minutes the absorbance was observed and recorded. The photocatalyst synthesized namely pristine TiO_2, HfO_2/TiO_2, and hydrogen annealed H-TiO_2, H-HfO_2/TiO_2 were dispersed in the solution. As shown in the Figure 6.10, before the start of each reaction, the solution vessel is kept in dark and stirred for about 10 minutes to disperse properly the photocatalyst. For all dyes, there is a particular wavelength at which highest absorption takes place and is set as the benchmark based on which all the other observations are recorded. The wavelengths corresponding for methylene blue is 590 nm and 440 nm each for thymol blue, cresol red, methyl orange and solochrome black.

As shown in Figure 6.10a and b, the pristine TiO_2 degradation for all the dyes was plotted and it was observed that the methylene blue was most degraded within a span of 30 mins after which it is saturated and little degradation takes place. For cresol red and methyl orange, the degradation was linear where the absorption was reduced linearly over time. Solochrome black and thymol blue absorption was reduced little during the whole process of reaction. Similar trends were observed for all the dyes where HfO_2/TiO_2 was used at photocatalyst as shown in Figure 6.10e and f.

Both hydrogenated samples showed better dye degradation activity. The hydrogenated TiO_2 and HfO_2/TiO_2 degraded quickly in 5 minutes itself compared to the air annealed counterpart which showed gradual degradation till 30 mins into the reaction (see Figure 6.10c, d and e, f). For solochrome black dye the degradation is showed most evidently by the H-HfO_2/TiO_2 which degraded completely by 25 minutes while for the other photocatalyst the degradation is limited and saturates after 10 minutes into the reaction. Thus, a sharp degradation is observed in methylene blue sample at the start of the reaction and the other dyes showed a gradual increase in degradation.

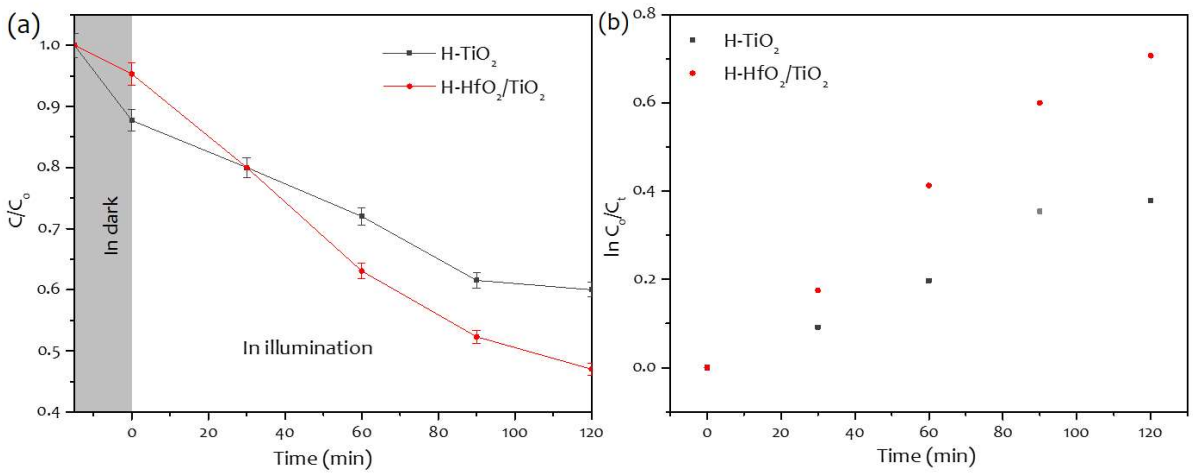

Figure 6.11 : Comparison of (a) photocatalytic activities and (b) rate constant of hydrogenated TiO_2 and HfO_2/TiO_2

The photo assisted water treatment by filter membrane with use of the hydrogenated samples of TiO_2 and HfO_2/TiO_2 are done for the removal Cr(VI) from water as shown in Figure 6.11a. The H-TiO_2 showed quicker degradation before illumination and during the first 20 minutes of the reaction. After which the conversion rate was similar for both the sample till 30 minutes in the reaction. But the H-HfO_2/TiO_2 sample showed increase in degradation efficiency and removed almost 50% after 120 minutes, whereas only 40% was removed by the H-TiO_2 sample. The H-HfO_2/TiO_2 showed high rate constant than the H-TiO_2 with 0.0061 min^{-1} and 0.0034 min^{-1} respectively (see Figure 6.11b). The reason for such condition might be because of the HfO_2 doping which provided light scattering effects increasing optical path length of all the incoming photons.

6.3 CONCLUDING REMARKS

This study gives a simple, cost effective and large scalability method to fabricate photo assisted catalytic material doped filter membrane. This photo catalytic filter membrane has a remarkable potential to photo-degrade harmful contaminates like Cr(IV) and industrial dyes and purify the water. With sub-zero temperature, photocatalytic membrane showed high rate constant and reported maximum degradation of Cr(IV). As excellent photocatalytic material for membrane, ZnO-TiO_2 heterojunction nanosphere exhibits no significant decrease degradation after several cycles. Also with high surface area, H-HfO_2/TiO_2 has successfully photodegraded the several industrial dyes like methyl orange, methylene blue, cresol red, solochrome black and thymol blue.